# Axisymmetric Shear Flow over Spheres and Spheroids

Arthur Rubel*
*Grumman Corporation, Bethpage, New York*

**Analytical solutions for an inviscid, incompressible, axisymmetric shear flow over a sphere are established. It is determined that if the shear is sufficiently large with respect to the axis velocity then a recirculating stagnation region is formed. Solutions for prolate and oblate spheroids exhibit the same flowfield characteristics as for the sphere. Stagnation bubble formation is delayed on the prolate spheroids and promoted on the oblate spheroids. These results are related to those for the two-dimensional shear flow over cylinders analyzed by Tsien (1943) and Fraenkel (1961).**

## Introduction

TSIEN[1] showed that when a cylinder is placed in a two-dimensional stream of constant shear that the stagnation point is displaced from the cylinder midpoint toward the side of greater freestream velocity. No stagnation bubble is present. Fraenkel[2] determined that when the stagnating streamline carries vorticity and is constrained to intersect the cylinder at its midpoint (e.g., by a wall) then a recirculation zone is established. The bubble closes at upstream infinity when the upstream velocity on the stagnating streamline vanishes and its size is reduced as the velocity is increased. Fraenkel noted that, in general, when the stagnating streamline makes an angle, $\beta$, with a body such that $\beta \leq \pi/2$, then the local stagnation point solution is dominated by a particular integral involving the vorticity. From the form of the solution he deduced that if the fluid included in angle $\beta$ possesses a velocity minimum on the stagnating streamline then a recirculation zone exists. In Tsien's problem, the displacement of the stagnating streamline precludes a stagnation bubble.

An axisymmetrically sheared flow was considered numerically by Rubel.[3] He found that, under certain conditions, the normal impingement of a round jet with a velocity minimum on its centerline produced recirculating stagnation regions. A local analysis verified the stagnation region characteristics but, unlike the two-dimensional case, no criteria for the bubble's appearance could be extracted.

In the work presented here, an axisymmetric shear flow about a sphere is investigated and, like the jet impact case, it is shown that stagnation bubbles make their appearance only after a critical dimensionless shear parameter is exceeded. The extent of these bubbles is consistent with that of Fraenkel's eddies on the cylinder; the reversed-flow zone closes at upstream infinity when the axis velocity vanishes. When cases are considered that include reversed flow at upstream infinity, then the axisymmetric solutions correspond to those two-dimensional solutions of Tsien on the low-velocity side of the cylinder.

The analytical results are extended to include the axisymmetric shear flow about prolate and oblate spheroids. Relative to the spherical results, the appearance of stagnation bubbles is promoted on oblate spheroids and delayed on prolate spheroids. When the oblate spheroid approaches the shape of a disk, the recirculation bubble takes a shape reminiscent of that calculated by Rubel[3] for jet impingement.

Received July 15, 1985; presented as Paper 85-1714 at the AIAA 18th Fluid Dynamics, Plasmadynamics and Lasers Conference, Cincinnati, OH, July 16-18, 1985. 

*Head, Theoretical Aerodynamics Laboratory, Corporate Research Center. Member AIAA.

## Analysis

### Spheres

Consider an axisymmetric shear flow that at $x \to -\infty$ has the form

$$u = u_0 - \frac{\Omega}{2} y^2, \qquad v = 0 \tag{1}$$

where $(u,v)$ are velocities in cylindrical $(x,y)$ coordinates (Fig. 1). Here $x$ is directed along the axis. The quantity $\Omega$ is related to the vorticity $\omega$ by

$$\frac{\omega}{y} = \frac{1}{y}\left(\frac{\partial v}{\partial x} - \frac{\partial u}{\partial y}\right) \equiv \Omega \tag{2}$$

If a stream function is defined in the usual manner, then

$$yu = \frac{\partial \psi}{\partial y}, \qquad -yv = \frac{\partial \psi}{\partial x} \tag{3}$$

and the equation for vorticity becomes

$$\frac{\partial^2 \psi}{\partial x^2} + y \frac{\partial}{\partial y}\left(\frac{1}{y}\frac{\partial \psi}{\partial y}\right) = -y^2 \Omega(\psi) \tag{4}$$

For axisymmetric steady flows, the quantity $\Omega(\psi)$ is fixed on stream surfaces and determined from upstream boundary values. Here $\Omega(\psi)$ is taken to be constant throughout the

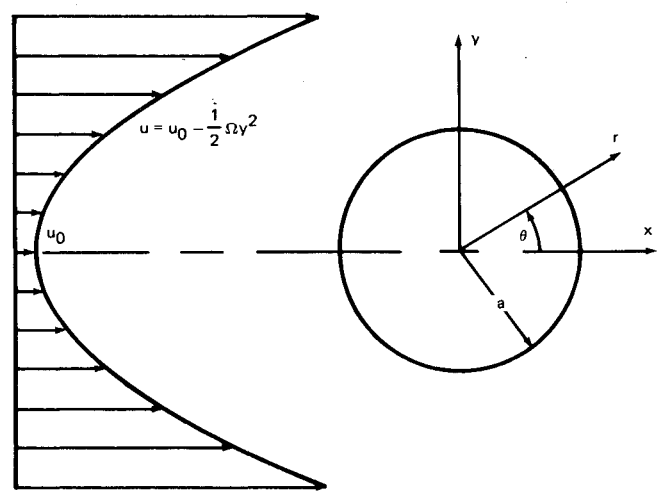


**Fig. 1 Schematic for axisymmetric shear flow over a sphere.**

flowfield. This is consistent with the upstream boundary constraints and satisfies the conditions of Batchelor[4] for closed stream surfaces in regions of inviscid axisymmetric flow.

The stream function $\psi_N$ obtained from Eqs. (1) and (3),

$$\psi_N = \frac{y^2}{2}\left(u_0 - \frac{\Omega y^2}{4}\right), \qquad x \to -\infty$$

is a nonhomogeneous solution to Eq. (4) considered herein to be satisfied at all points far from the sphere.

To consider the flow about the sphere it is convenient to use spherical polar coordinates $(r,\theta)$, where

$$y = r\sin\theta, \qquad x = r\cos\theta$$

Velocities are defined accordingly, i.e.,

$$v = q_r\sin\theta + q_\theta\cos\theta, \qquad u = q_r\cos\theta - q_\theta\sin\theta$$

where

$$q_r = \frac{1}{r^2\sin\theta}\frac{\partial\psi}{\partial\theta}, \qquad q_\theta = -\frac{1}{r\sin\theta}\frac{\partial\psi}{\partial r}$$

The governing equation becomes

$$\frac{\partial^2\psi}{\partial r^2} + \frac{\sin\theta}{r^2}\frac{\partial}{\partial\theta}\left(\frac{1}{\sin\theta}\frac{\partial\psi}{\partial\theta}\right) = -\Omega r^2\sin^2\theta \tag{5}$$

and the nonhomogeneous solution is

$$\psi_N = \frac{1}{2}r^2\sin^2\theta\left(u_0 - \frac{\Omega}{4}r^2\sin^2\theta\right) \tag{6}$$

In order to satisfy the boundary condition $\psi = 0$ on the sphere of radius $a$, a solution to the homogeneous governing equations $\psi_H$ is required such that

$$\psi = \psi_N + \psi_H$$

with

$$\psi_N(a,\theta) + \psi_H(a,\theta) = 0 \quad \text{and} \quad \psi_H(\infty,\theta) = 0$$

Solutions of the required form are related to the zonal harmonic functions; namely,

$$\psi_H = \sin^2\theta\sum_{n=1} A_n P_n'(\cos\theta) r^{-n} \tag{7}$$

where $P_n'$ is the derivative of the Legendre function of the first kind of order $n$. The coefficients satisfying the boundary condition at $r = a$ are found to be

$$A_1 = -a^3\left(\frac{u_0}{2} - \frac{a^2\Omega}{10}\right)$$

$$A_3 = -\frac{a^7\Omega}{60}$$

$$A_n = 0, \quad n \neq 1,3$$

The full solution is

$$\psi = \frac{u_0}{2}r^2\sin^2\theta\left(1 - \frac{a^3}{r^3}\right) - \frac{\Omega r^4}{8}\sin^2\theta\left[\left(1 - \frac{a^7}{r^7}\right)\sin^2\theta - \frac{4}{5}\frac{a^5}{r^5}\left(1 - \frac{a^2}{r^2}\right)\right] \tag{8}$$

In dimensionless form, Eq. (8) becomes

$$\Psi = \left[\Lambda R^2(1 - R^{-3}) + \frac{4}{5}R^{-1}(1 - R^{-2})\right]\sin^2\theta - R^4(1 - R^{-7})\sin^4\theta \tag{9}$$

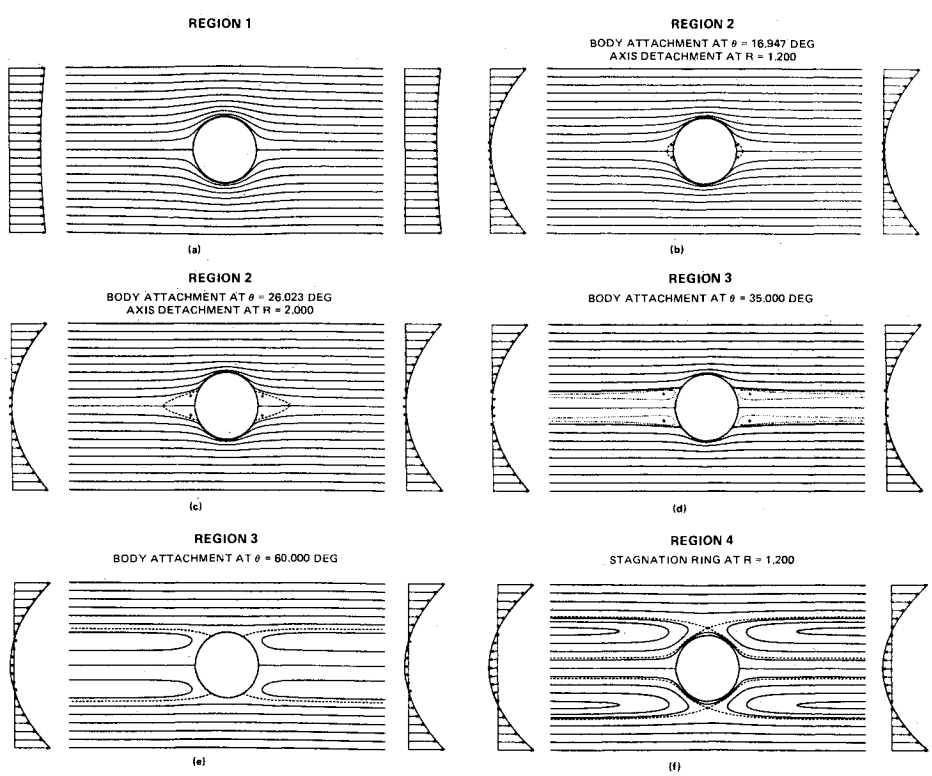


**Fig. 2 Flow over a sphere; stream surfaces. Λ = a) −93.333, b) −0.336, c) −0.086, d) 0.232, e) 1.213, f) 2.507.**

with $R=r/a$, $\Lambda=4u_0/\Omega a^2$, and $\Psi=8\psi/\Omega a^4$. $\Lambda$ may be regarded as the reciprocal of a dimensionless vorticity parameter.

Inherent in this form for $\Psi$ are the zeros that appear at $R=1$ and $\theta=0,\pi$. If these roots are extracted,

$$\frac{\Psi}{(1-R^{-1})\sin^2\theta}=\Lambda R^2(1+R^{-1}+R^{-2})+\frac{4}{5}R^{-1}(1+R^{-1})$$

$$-(1+R^{-1}+R^{-2}+R^{-3}+R^{-4}+R^{-5}+R^{-6})R^4\sin^2\theta$$

and when this function vanishes at $R=1$ or $\theta=0,\pi$, a dividing stream surface must exist. At such locations

$$\sin^2\theta=\Lambda R^2(R^2+R+1)+\frac{4}{5}(R+1)$$

$$\div(R^6+R^5+R^4+R^3+R^2+R+1) \qquad (10)$$

and solutions to Eq. (10) serve to categorize four classes of flow in terms of the parameter $\Lambda$.

For $\Lambda<-8/15$ there is no solution to Eq. (10) for which $R=1$ or $\theta=0,\pi$. This is a region in which the irrotational features of the solution are dominant and the result resembles a potential flow about the sphere (Fig. 2a). A single stagnation point is present on the $x<0$ half of the sphere.

As $\Lambda$ is increased so that $-8/15<\Lambda<0$, Eq. (10) has solutions for $\theta=0,\pi$ as well as for $R=1$. These solutions represent the separation and reattachment points, respectively, of the stagnation bubbles. The bubbles appear as $\Lambda$ is increased beyond $\Lambda=-8/15$ (Fig. 2b) and their size increases with $\Lambda$ (Fig. 2c) until the separation point approaches upstream infinity at $\Lambda\to 0$. In these figures the crosses denote the location of internal stagnation points (i.e., within the bubbles), and the dividing stream surfaces are indicated by the dashed lines.

Examples for $\Lambda>0$ imply reversed flow at $x=\pm\infty$. For $0<\Lambda<9/5$, solutions exist to Eq. (10) when $R=1$. As $\Lambda$ is increased from zero, the reattachment stagnation ring moves toward the top of the sphere (Figs. 2d and 2e). The region of reversed flow is confined within the dividing stream surface. As $\Lambda$ is increased from zero, the separated flow bubble detaches from the sphere and its axis to form an annular-shaped bubble (dotted dividing stream surface of Fig. 2d) immersed within the region of reversed flow. This bubble is closed at upstream infinity at the location of vanishing velocity, i.e., where $y/a=\sqrt{\Lambda/2}$. An analysis of internal stagnation point locations (i.e., $\partial\Psi/\partial R=\partial\Psi/\partial\theta=0$; $R>1$, $\theta\neq 0,\pi$) shows that these points approach $y/a=\sqrt{\Lambda/2}$ for $\Lambda\to 4/5$. Hence, no bubbles appear for $\Lambda>4/5$.

At $\Lambda=9/5$ ($\theta=\pi/2$, $R=1$) the dividing stream surface detaches from the top of the sphere and, for $\Lambda>9/5$, a second dividing surface appears (Fig. 2f). There is flow across the $x=0$ plane in both directions separated by an off-body stagnation ring. Considering the $x<0$ region, streamlines trapped between the dividing stream surfaces enter and exit from upstream infinity and a single stagnation point exists on the half sphere. The $\Lambda>0$ cases are the axisymmetric analogs of the two-dimensional reversed-flow regions about a cylinder in a constant shear flow.[1] However, no regions of closed stream surfaces appear in the two-dimensional case.

The velocity distribution on the sphere (scaled by the maximum velocity) is greatly dependent upon the value of $\Lambda$ (Fig. 3). For $\Lambda\to-\infty$ the potential flow distribution is recovered. As $\Lambda$ is increased, the velocity slows in the stagnation region until at $\Lambda=-8/15$, a second stagnation region appears and the velocity changes sign on the sphere. Further increases in $\Lambda$ cause the second stagnation point to move toward the $\theta=\pi/2$ point with increasing regions of reversed flow. For $\Lambda>9/5$ the entire sphere is immersed in a reversed flow and as $\Lambda\to-\infty$ the potential solution is again recovered.

### Spheroids

Some effects of body shape on the flow structure can be examined by considering spheroids to be immersed in the shear flow given by Eq. (1). Following Lamb,[5] the elliptic coordinates given implicitly by

$$x=k\mu\zeta,\quad y=k(1-\mu^2)^{1/2}(\zeta^2\pm 1)^{1/2} \qquad (11)$$

are convenient for the description of the flowfield. Here, constant $\zeta,\mu$ define confocal ellipsoids and hyperboloids with common foci at a distance $k$ from the origin; the $\pm$ refers to oblate and prolate spheroids, respectively. The body is given by

$$c=k\zeta_0,\quad a=k(\zeta_0^2\pm 1)^{1/2},\quad e^2=1-(c/a)^{\pm 2} \qquad (12)$$

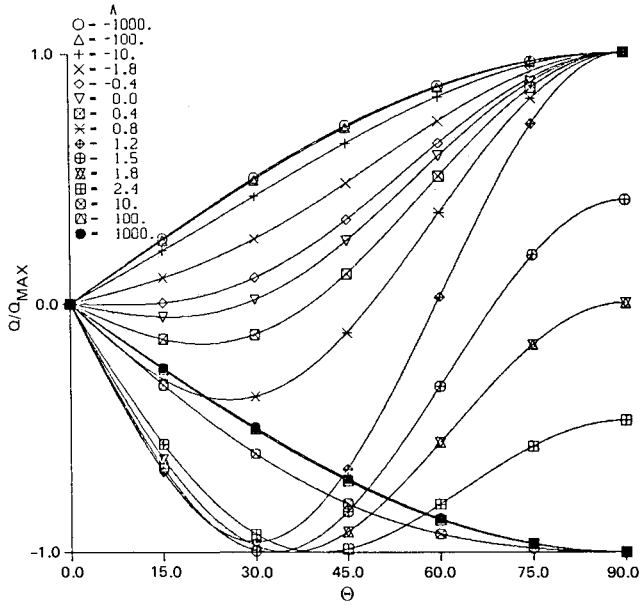


Fig. 3 Velocity distribution over a sphere.

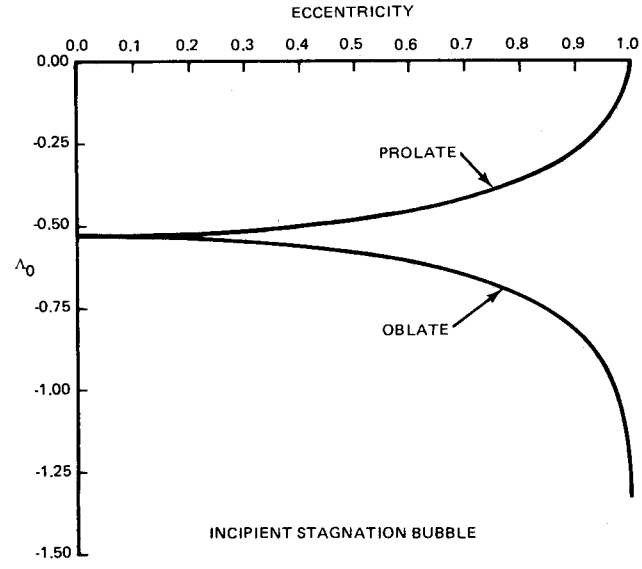


Fig. 4 Dependence of separation bubble formation on spheroid eccentricity.

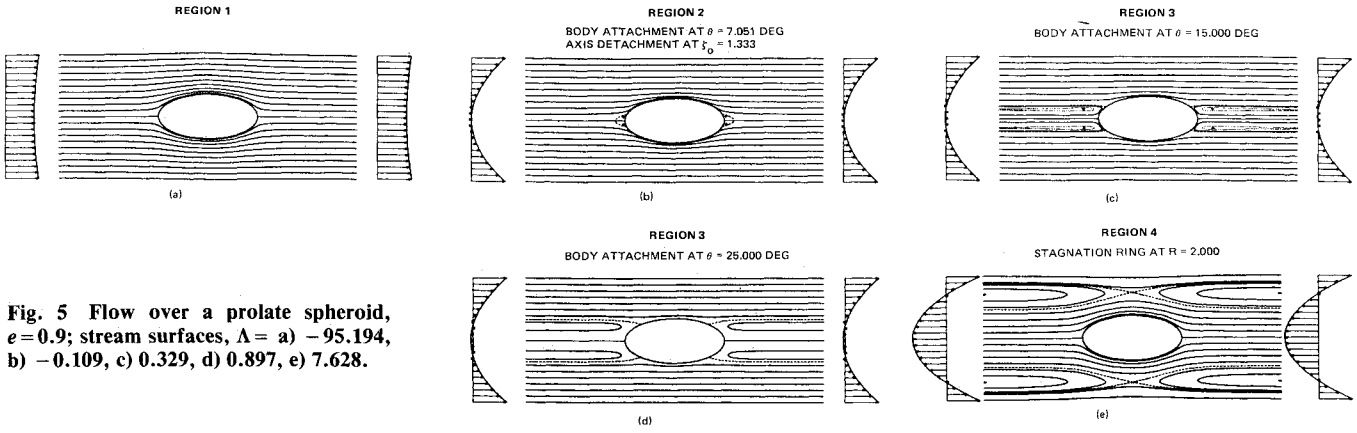


**Fig. 5 Flow over a prolate spheroid, $e=0.9$; stream surfaces, $\Lambda=$ a) $-95.194$, b) $-0.109$, c) 0.329, d) 0.897, e) 7.628.**

**Table 1 $\Lambda_0$ and $\Lambda_D$ for limiting spheroid cases**

| | Prolate "needle" $\zeta_0 \to 1$ | Sphere $\zeta_0 \to \infty$ | Oblate "disk" $\zeta_0 \to 0$ |
|---|---|---|---|
| $\Lambda_0$ | 0 | $-8/15$ | $-4/3$ |
| $\Lambda_D$ | 2 | 9/5 | 4/3 |

where $c$ and $a$ define the extent of the body measured from the origin along and normal to the axis, respectively. The eccentricity of the ellipse is given by $e$, while $k$ acts as a scale factor and $\zeta_0$ defines the body coordinate. For the prolate spheroid $1<\zeta<\infty$, while, for the oblate spheroid, $0<\zeta<\infty$; in either case, $-1\le\mu\le 1$. The spheroids approach the spherical shape when $e\to 0$ or $\zeta_0\to\infty$.

In these coordinates, transformation of Eq. (4) provides the governing equation for the stream function, viz.,

$$\frac{1}{(1-\mu^2)}\frac{\partial^2\psi}{\partial\zeta^2}+\frac{1}{(\zeta^2\pm 1)}\frac{\partial^2\psi}{\partial\mu^2}=-k^4(\zeta^2\pm\mu^2)\Omega(\psi) \quad (13)$$

The velocities are defined by

$$q_\zeta=\frac{1}{k^2(\zeta^2\pm\mu^2)^{1/2}(\zeta^2\pm 1)^{1/2}}\frac{\partial\psi}{\partial\mu}$$

$$q_\mu=-\frac{1}{k^2(\zeta^2\pm\mu^2)^{1/2}(1-\mu^2)^{1/2}}\frac{\partial\psi}{\partial\zeta}$$

The nonhomogeneous solution of Eq. (13) is again satisfied by Eq. (6), or

$$\psi_N=\tfrac{1}{2}k^2(1-\mu^2)(\zeta^2\pm 1)\left[u_0-\frac{\Omega k^2}{4}(1-\mu^2)(\zeta^2\pm 1)\right] \quad (14)$$

so that the boundary condition $\psi=0$ on the spheroid requires the homogeneous solution $\psi_H$, such that

$$\psi=\psi_N+\psi_H$$

with

$$\psi_H=k\sum_{n=1}\frac{A_n}{n(n+1)}(1-\mu^2)P_n'(\mu)(\zeta^2\pm 1)Q_n'(\bar\zeta) \quad (15)$$

where $Q_n'$ is the derivative of the Legendre function of the second kind of order $n$. The argument $\bar\zeta$ is given by $\bar\zeta=\zeta$ or $i\zeta$ for the prolate and oblate cases, respectively. The coefficients satisfying the boundary condition at $\zeta=\zeta_0$ are found to be

$$A_1=\frac{k}{Q_1'(\bar\zeta_0)}\left[-u_0+\frac{1}{5}k^2\Omega(\zeta_0^2\pm 1)\right]$$

$$A_3=-\frac{k^3\Omega(\zeta_0^2\pm 1)}{5Q_3'(\bar\zeta_0)}$$

$$A_n=0, \quad n\neq 1,3$$

so that the full solution is

$$\psi=-\frac{1}{2}k^2(1-\mu^2)(\zeta^2\pm 1)\left\{u_0[1-S_1(\zeta,\zeta_0)]+\frac{k^2\Omega}{4}(\zeta_0^2\pm 1)\left((1-\mu^2)[1-S_2(\zeta,\zeta_0)]-\left(\frac{1}{5}-\mu^2\right)[1-S_3(\zeta,\zeta_0)]-\frac{4}{5}[1-S_1(\zeta,\zeta_0)]\right)\right\} \quad (16)$$

where

$$S_1(\zeta,\zeta_0)=Q_1'(\bar\zeta)/Q_1'(\bar\zeta_0) \quad (17a)$$

$$S_2(\zeta,\zeta_0)=(\bar\zeta^2-1)/(\bar\zeta_0^2-1) \quad (17b)$$

$$S_3(\zeta,\zeta_0)=Q_3'(\bar\zeta)/Q_3'(\bar\zeta_0) \quad (17c)$$

Evaluation of Eqs. (17) for $S_1$, $S_2$, $S_3$ yields different functional forms (in terms of $\zeta$) for prolate and oblate spheroids. In dimensionless form, Eq. (16) becomes

$$\Psi=\frac{(1-\mu^2)(\zeta^2\pm 1)}{(\zeta_0^2\pm 1)}\left\{\Lambda[1-S_1(\zeta,\zeta_0)]+(1-\mu^2)[1-S_2(\zeta,\zeta_0)]-\left(\frac{1}{5}-\mu^2\right)\times[1-S_3(\zeta,\zeta_0)]-\frac{4}{5}[1-S_1(\zeta,\zeta_0)]\right\} \quad (18)$$

where $\Lambda$ and $\Psi$ retain their previous definitions, and the length scale $a$ is still equal to the radius of the body at the origin.

The zeros of the curly bracket of Eq. (18) define the dividing stream surface. Hence, the expression

$$1-\mu^2=\left[\frac{4}{5}(S_3-S_1)+\Lambda(S_1-1)\right]\Big/(S_3-S_2) \quad (19)$$

serves to define the regions of flow over the spheroids. The arguments of the $S$ functions have been dropped for convenience.

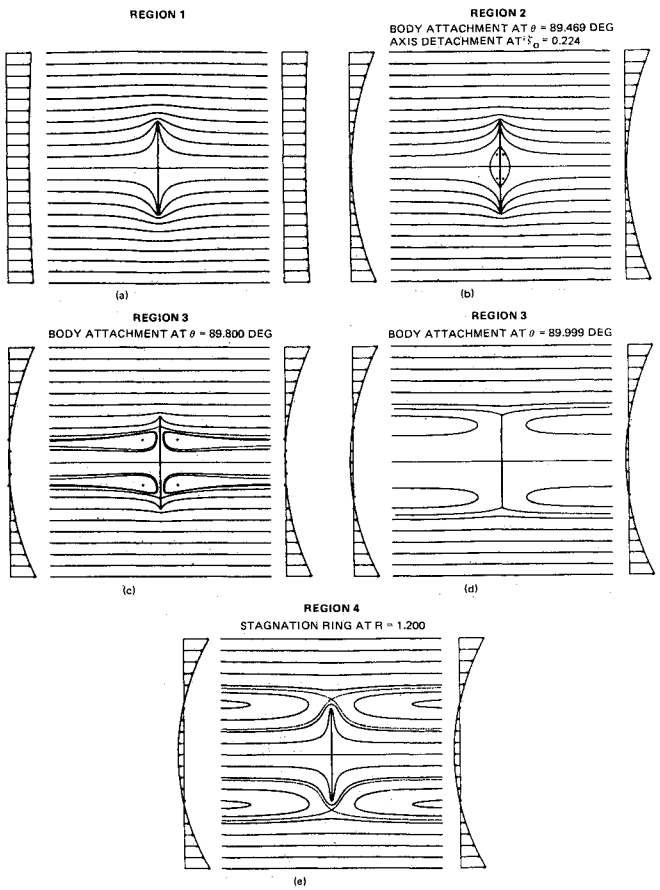


**Fig. 6 Flow over an oblate spheroid (disk), $e=0.99999$; stream surfaces, $\Lambda=$ a) $-99.414$, b) $-0.790$, c) 0.330, d) 1.338, e) 2.398.**

If a stagnation bubble is to appear, then Eq. (19) must be satisfied on the axis (i.e., $\mu=\pm 1$). Furthermore, when the bubble is just about to appear $\zeta\to\zeta_0$. Defining $\Lambda_0$ as the $\Lambda$ of incipient bubble appearance,

$$\Lambda_0=\left[\frac{4}{5}(S_3-S_1)\Big/(1-S_1)\right]_{\zeta\to\zeta_0}=\frac{4}{5}(1-S'_{30}/S'_{10}) \quad (20)$$

where $S'_{10}$ and $S'_{30}$ indicate derivatives of $S_1$ and $S_3$ with respect to $\zeta$, respectively, evaluated at $\zeta=\zeta_0$. No bubbles are possible when $\Lambda<\Lambda_0$.

The solution to Eq. (20) has been found for the entire range of spheroid eccentricity (Fig. 4). [Equation (12) may be used to relate $\zeta_0$ to the eccentricity.] For eccentricity approaching zero the $\Lambda_0\to -8/15$ value of the sphere is recovered. As the spheroid becomes more oblate, $\Lambda_0$ is increasingly negative (i.e., separation is promoted) until the limiting case $\Lambda_0\to -4/3$ for $e\to 1$. For prolate spheroids the magnitude of $\Lambda_0$ is reduced until the limiting case $\Lambda_0\to 0$ for $e\to 1$. This result is not surprising in view of the spherical results. When a separation bubble appears in front of the sphere (Figs. 2b and 2c), it presents a dividing stream surface more prolate in nature and allows the flow to pass about the sphere.

As $\Lambda$ is increased from $\Lambda_0$ the bubbles increase in size until the axis separation point approaches infinity as $\Lambda\to 0$. The value of $\mu$ that satisfies Eq. (19) for $\Lambda>\Lambda_0$, $\zeta=\zeta_0$ defines the attachment of the dividing stream surface to the body. Reversed flow exists at upstream infinity when $\Lambda>0$. The limiting case of $\mu\to 0$ coincides with the dividing stream about to detach from the spheroid. If, for detachment, $\Lambda$ is defined by $\Lambda_D$ then, from Eq. (19),

$$\Lambda_D=1-\tfrac{1}{4}\Lambda_0-S'_{20}/S'_{10} \quad (21)$$

Values of the separating and detachment $\Lambda$ are given here for limiting spheroid cases.

In each case in Table 1 the character of the flow is determined by the value of $\Lambda$, so that $\Lambda<\Lambda_0$, potential-like flow; $\Lambda_0<\Lambda<0$, separation bubbles; $0<\Lambda<\Lambda_D$, reversed flow upstream, attachment at the body; and $\Lambda_D<\Lambda$, reversed flow over the entire body.

The flowfield about a prolate spheroid (Fig. 5) and oblate disk (Fig. 6) exhibits the same qualitative features as the flow over a sphere. Note the low magnitude of $\Lambda=-0.109$ required to produce a small bubble on the $e=0.9$ prolate spheroid (Fig. 5b) in contrast to $\Lambda=-0.790$ for the case of an oblate disk (Fig. 6b). The bubble produced on the disk bears a striking resemblance to the bubble calculated numerically by Rubel[3] for jet impingement on a flat plate. Another feature of these flows is that the bubble within the reversed-flow region (dotted line, Figs. 5c and 6c) appears for $\Lambda>0$ and disappears at $\Lambda=4/5$ independent of the eccentricity. This requires an analysis of the internal stagnation point locations (i.e., $\partial\psi/\partial\zeta=\partial\psi/\partial\mu=0$; $\zeta>\zeta_0$, $\mu\neq 0,\pm 1$) for $\zeta\to\infty$. Note that the reattachment of the dividing stream surface for $\Lambda=1.338$ on the oblate disk (Fig. 6d) is almost coincident with the limiting detachment value $\Lambda=4/3$ for $\zeta_0\to 0$.

## Concluding Remarks

An inviscid, axisymmetric shear flow about a spheroid can be classified by the value of the parameter $\Lambda=4u_0/\Omega a^2$. Unlike the two-dimensional shear flow about a half-cylinder,[2] there is a shear threshold below which stagnation bubbles do not appear. This result is in agreement with numerical results reported for axisymmetric jet impingement on a plane wall.[3] In fact, the stagnation bubbles analyzed here, for flow over an oblate disk, possess dividing stream surfaces reminiscent of those jet impingement computations. When the value of $\Lambda\to 0$ (e.g., $u_0\to 0$ or $\Omega\to-\infty$), the separated flow zone becomes infinite in extent, much like the two-dimensional eddies of Fraenkel.[2] Solutions for prolate and oblate spheroids exhibit the same flowfield characteristics as for the sphere. Stagnation bubble formation is delayed on prolate spheroids and promoted on oblate spheroids.

## References

[1]Tsien, H. S., "Symmetrical Joukowsky Airfoils in Shear Flow," *Quarterly of Applied Mathematics*, Vol. 1, 1943, p. 130.

[2]Fraenkel, L. E., "On Corner Eddies in Plane Inviscid Shear Flow," *Journal of Fluid Mechanics*, Vol. 11, 1961, p. 400.

[3]Rubel, A., "Inviscid Axisymmetric Jet Impingement with Recirculating Stagnation Regions," *AIAA Journal*, Vol. 21, March 1983, pp. 351-357.

[4]Batchelor, G. K., "On Steady Laminar Flow with Closed Streamlines at Large Reynolds Number," *Journal of Fluid Mechanics*, Vol. 1, 1956, p. 177.

[5]Lamb, H., *Hydrodynamics*, 6th Ed., Dover Publications, New York, 1932, pp. 139-146.